remote sensing

MDPI

Article

Enhancing Identification of Meteorological and Biological Targets Using the Depolarization Ratio for Weather Radar: A Case Study of FAW Outbreak in Rwanda

Fidele Maniraguha [1,2,*], Anthony Vodacek [3], Kwang Soo Kim [4], Emmanuel Ndashimye [1,5] and Gerard Rushingabigwi [1,6]

[1] African Center of Excellence in Internet of Things, University of Rwanda, KN 67 Street, Kigali P.O. Box 3900, Rwanda; endashim@andrew.cmu.edu (E.N.); g.rushingabigwi@ur.ac.rw (G.R.)
[2] Technology and Information System Division, Rwanda Meteorology Agency, KN 96 Street, Kigali P.O. Box 898, Rwanda
[3] Chester F. Carlson Center for Imaging Science, Rochester Institute of Technology, Rochester, NY 14623, USA; axvpci@rit.edu
[4] Department of Agriculture, Forestry and Bioresources, Seoul National University, Seoul 08826, Republic of Korea; luxkwang@snu.ac.kr
[5] Department of Information and Communication Technology, Carnegie Mellon University Africa, Kigali 10000, Rwanda
[6] Department of Electrical and Electronic Engineering (EEE), University of Rwanda, KN 67 Street, Kigali P.O. Box 3900, Rwanda
* Correspondence: manifils@gmail.com

Abstract: Leveraging weather radar technology for environmental monitoring, particularly the detection of biometeors like birds, bats, and insects, presents a significant challenge due to the dynamic nature of their behavior. Unlike hydrometeor targets, biometeor targets exhibit arbitrary changes in direction and position, which significantly alter radar wave polarization upon scattering. This study addresses this challenge by introducing a novel methodology utilizing Rwanda's C-Band Polarization Radar. Our approach exploits the capabilities of dual-polarization radar by analyzing parameters such as differential reflectivity (ZDR) and correlation coefficient (RHOHV) to derive the Depolarization Ratio (DR). While existing radar metrics offer valuable insights, they have limitations in fully capturing depolarization effects. To address this, we propose an advanced fuzzy logic algorithm (FL_DR) integrating the DR parameter. The FL_DR's performance was rigorously evaluated against a standard FL algorithm. Leveraging a substantial dataset comprising nocturnal clear air radar echoes collected during a Fall Armyworm (FAW) outbreak in maize fields from September 2020 to January 2021, the FL_DR demonstrated a notable improvement in accuracy compared to the existing FL algorithm. This improvement is evident in the Fraction of Echoes Correctly Identified (FEI), which increased from 98.42% to 98.93% for biological radar echoes and from 87.02% to 95.81% for meteorological radar echoes. This enhanced detection capability positions FL_DR as a valuable system for monitoring, identification, and warning of environmental phenomena in regions similar to tropical areas facing FAW outbreaks. Additionally, it could be tested and further refined for other migrating biological targets such as birds, insects, or bats.

Keywords: depolarization ratio (DR); fuzzy logic algorithm; fall armyworm (FAW) detection; weather radar; FAW early warning system

Citation: Maniraguha, F.; Vodacek, A.; Kim, K.S.; Ndashimye, E.; Rushingabigwi, G. Enhancing Identification of Meteorological and Biological Targets Using the Depolarization Ratio for Weather Radar: A Case Study of FAW Outbreak in Rwanda. *Remote Sens.* **2024**, *16*, 2509. https://doi.org/10.3390/rs16142509

Academic Editor: Silas Michaelides

Received: 30 May 2024
Revised: 24 June 2024
Accepted: 27 June 2024
Published: 9 July 2024

1. Introduction

Monitoring airborne insects in Africa, especially agricultural pests like Fall Armyworms, faces challenges due to resource limitations and technological disparities compared to more developed regions such as Europe and North America [1–3]. While weather radars in these advanced areas offer valuable insights into insect behavior and migration which

aids pest management and ecological research [4,5], financial constraints and technological and skills gaps in Africa hinder the acquisition and maintenance of such monitoring systems. This results in an incomplete understanding of airborne biological movements in the continent's diverse ecosystems.

The Fall Armyworm (*Spodoptera frugiperda*) emerged as a significant threat to African agriculture in 2016 upon its introduction to West and Central Africa, swiftly spreading across numerous countries, including Rwanda [6,7]. The first sighting of FAW in Rwanda occurred in February 2017, in the maize fields of Mushishito marshland located in the Nyamagabe district of the southern province [8,9]. This infestation caused extensive damage to maize and sorghum crops, crucial for food security in Rwanda and Sub-Saharan Africa. Throughout the agricultural season from September 2020 to January 2021, outbreaks of FAW were reported, affecting 1160 hectares of maize fields in the Nyanza, Huye, and Gisagara Districts. The initial infestation report in October 2020 impacted over 280 hectares [10].

Biometeors, including insects, exhibit distinct radar signatures that set them apart from meteorological phenomena. These signatures typically include low horizontal reflectivity (DBZH), ranging from −10 to 35 dBZ; high differential reflectivity (ZDR) due to their elongated shapes, with values reaching up to +7 dB; a relatively low correlation coefficient (RHOHV) compared to meteorological echoes, generally below 0.86; and a relatively high differential phase (KDP) for hydrometeors compared to biometeors. However, large numbers of airborne insects in flight can result in very high RHOHV values, up to 0.96, often leading weather radar algorithms to mistakenly classify them as precipitation [9,10].

In our previous study [10], a fuzzy logic algorithm incorporating DBZH, ZDR, RHOHV, and KDP as inputs was utilized to establish thresholds and signatures for detecting and classifying FAW amidst an outbreak and infestation of maize crop fields in three districts of Rwanda's southern province from September 2020 to January 2021. This approach yielded promising results in the early detection of adult FAW arrival in the infested area, highlighting a strong connection between radar insect echoes detected over areas of FAW infestation in maize fields across the monitored districts during the infestation period. Additionally, trends in insect echoes during and before the infestation suggest the potential of weather radar as a tool for monitoring and early warning of FAW. However, there is room for improvement in detection and classification performance by integrating new parameters, such as Depolarization Ratio, which incorporates the depolarization impacts from biological airborne targets. To enhance this methodology, a new fuzzy logic algorithm, which integrates the DR parameter (FL_DR), is proposed and tested in this study, employing similar approaches and data samples as those used in the preceding research.

Building upon these results and inspired by Kilambi et al.'s methodology [11,12], which proposed a technique for distinguishing weather echoes from non-weather targets using the DR parameter derived from RHOHV and ZDR, we integrate the derived DR parameter into FL, creating a new FL_DR method with five polarimetric radar parameters (DBZH, ZDR, RHOHV, KDP, and DR). This DR integration not only seeks to improve the accuracy of classifying both meteorological and biological targets but also expands our research scope with a prime focus on distinguishing between weather and biological targets, particularly for classifying the FAW outbreak.

Objects like insects exhibit distinct scattering behaviors in weather radar data due to their irregular shapes and varying orientations, leading to significant depolarization and larger absolute values of ZDR ($|ZDR|$) compared to typical meteorological targets, such as rain particles, which tend to have more spherical shapes. The depolarization term ($|ZDR|$) in the DR equation dominates the numerator for insects, resulting in a smaller DR value compared to other scatterers, highlighting the sensitivity of DR to the specific depolarization characteristics associated with different target types.

Separating biological and meteorological echoes is challenging due to the wide range of radar parameters like DBZH, ZDR, KDP, and RHOHV. This variability can lead radar algorithms to misidentify biological echoes as precipitation, resulting in classification errors even with advanced algorithms [13–15]. These challenges hinder precise target classification

and limit the effectiveness of traditional approaches. In contrast, fuzzy logic emerges as a promising alternative for weather radar data analysis, as it embraces uncertainties inherent in real-world scenarios and allows for partial membership in target classes. One notable strength of fuzzy logic is its utilization of membership functions as adaptable filters to remove echo pixels that are well outside the target signatures, followed by a nuanced classification process tailored to match the characteristics of various targets within retained radar pixels. This flexibility enables fuzzy logic to provide a more nuanced and potentially more accurate method for analyzing radar data, especially in detecting biometeors like insects [16–18].

This adaptability allows for more refined and precise classifications, accommodating the diverse nature of airborne particles. Additionally, fuzzy logic facilitates the simultaneous analysis of multiple airborne objects within a single dataset, providing a comprehensive understanding of atmospheric conditions. By considering interactions among different types of airborne particles, fuzzy logic enhances decision-making across various applications, from weather forecasting to environmental monitoring. This holistic approach supports more informed decisions and improves the overall understanding of atmospheric phenomena [11,19].

Despite its advantages, fuzzy logic algorithms are not without limitations. One significant issue arises when membership function values overlap, leading to erroneous identifications [10,20,21]. To mitigate this, subjective conditions in the form of threshold values based on membership function curves are often imposed. However, this introduces a level of arbitrariness that can impact the reliability and accuracy of classifications. The selection of appropriate membership functions, such as gaussian, trapezoidal, and triangular shapes, is crucial, as they significantly influence the system's performance and overall effectiveness in handling uncertain real-world problems [10,20].

Recent advancements in weather radar technology, such as the Simultaneous Transmission and Reception (SHV) mode, have significantly enhanced our ability to classify atmospheric targets by providing valuable data through parameters like ZDR and RHOHV [22]. However, the SHV mode has limitations in fully capturing the phenomenon of depolarization, which describes how targets alter wave polarization [23]. This is where the Depolarization Ratio (DR) becomes crucial, offering a deeper understanding of depolarization effects, especially for dynamic targets like biometeors [24].

Before the SHV mode became dominant, radars used circular polarization. Circular Depolarization Ratio (CDR) was especially important in aviation radars for mitigating weather echo contamination [23,25,26]. This was due to a key characteristic of weather particles: their uniform shape (high RHOHV) and near-spherical form (ZDR $\approx$ 1 in linear units), which distinguished them from other objects. However, modern radars cannot directly measure CDR because of the inherent nature of SHV transmission [11,24,26].

Linear Depolarization Ratio (LDR) was developed to measure depolarization directly [27]. While LDR provided useful measurements, it required a dedicated polarization switch, leading to drawbacks like slower data updates and switch wear, limiting its widespread adoption. To overcome these challenges, researchers introduced Depolarization Ratio (DR) as a proxy for both CDR and LDR. Formulated using existing the SHV mode measurements (DBZH and RHOHV), DR provides valuable insights into depolarization effects without the need for a separate LDR mode [11,24,26].

2. Materials and Methods

2.1. Meteo Rwanda Weather Radar Data

Similar to our prior study [10], radar data utilized in this study are collected by Meteo Rwanda, employing a Polarimetric C-Band dual Doppler weather radar system stationed in the Bugesera district, eastern province, since 2015 (Figure 1). This weather radar system is equipped with dual-polarization capabilities, facilitating simultaneous transmission and reception for comprehensive weather data collection. It measures numerous polarimetric parameters, including DBZH, RHOHV, ZDR, KDP, among others. Despite the Meteo

Rwanda radar not automatically generating the DR, it is computed following methodologies proposed by various researchers from ZDR and RHOHV for all elevation angles [11,22,24,28]. The DR calculation process is automated to ensure continuous real-time calculation during radar operation.

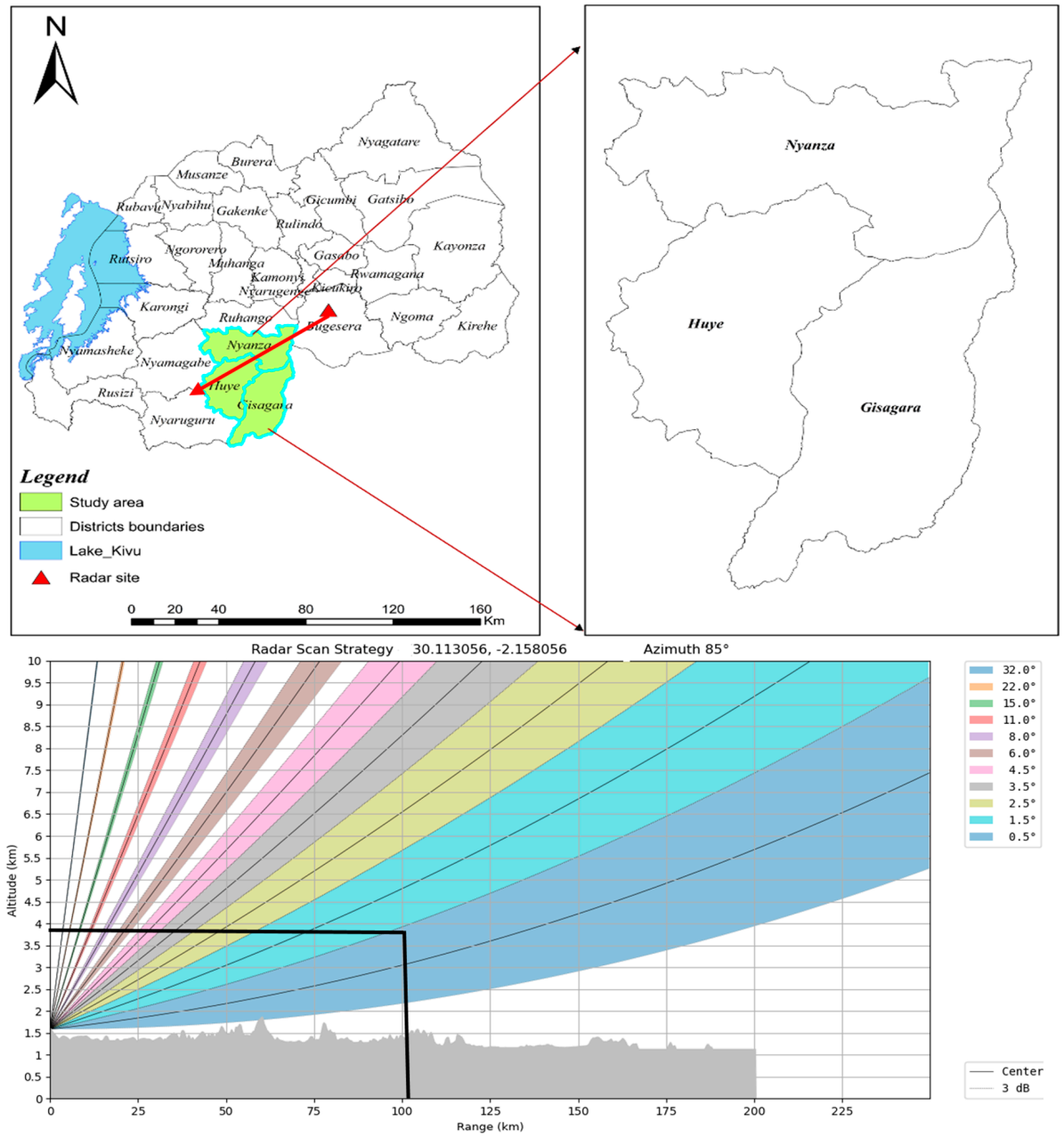

Figure 1. Study area and Meteo Rwanda weather radar scan strategy, with the red arrow pointing southwest at 2250 toward the study area, showing a clear view with no beam blockage.

The Meteo Rwanda radar operates with a 1° beam width and conducts 11 azimuthal scans from 0.5° to 32.0° elevation angles, covering a maximum range of 250 km [10,29]. The raw radar data are processed in the Thunderstorm Identification, Tracking, Analysis, and Nowcasting (TITAN) environment [17]. TITAN uses dual Doppler weather radar parameters with fuzzy logic to identify storm particle size and shape. Within TITAN, fuzzy logic membership functions are developed to differentiate between various hydrometeor particles such as rain, hail, and snow, leveraging multiple variables and independent features [30,31].

However, despite the radar being installed in 2015, the data archive starts from November 2017. This gap in the radar data makes it impossible to monitor insect abundance prior to the first sighting of Fall Armyworm (FAW) in Rwanda in February 2017 [8]. Consequently, this lack of earlier data prevents from analyzing the conditions and potential warning signs leading up to the FAW's appearance, which could have provided valuable insights for early detection and prevention strategies.

2.2. Ground Reference FAW Outbreak Data

Ground observation data on FAW outbreaks and maize infestations from three districts (Nyanza, Huye, and Gisagara) form the foundation and reference for this research, as detailed in our previous study [10]. This retrospective study relies on FAW outbreak observations recorded by the Rwanda Agriculture Board (RAB) Rubona station. Field data were collected from 1160 hectares of maize fields in these districts, with farmers reporting infestations by sighting caterpillars and observing adult moth movements. As FAW are nocturnal, these observations were typically made after sunset and before sunrise in the early morning. During the day, farmers could only see the damage caused by the larvae (or caterpillars). The data collected are crucial for understanding the spread and impact of FAW, providing valuable insights into infestation patterns and timing. Additionally, these observations help inform the correlation between ground and radar observations, contributing to the development of effective identification algorithms.

Initial monitoring in October 2020 revealed FAW presence among 156 farmers, with the situation worsening within five weeks of planting, affecting over 280 hectares, highlighting the severity of FAW infestations [10]. Additionally, this study incorporates nocturnal clear air weather radar data collected over infested maize fields during the infestation period. It is assumed that night clear air echoes over these fields and marshlands primarily originate from insects rather than birds, considering the unimodal pattern of tropical regional bird activity and foraging concentrated towards the end of the day [32,33]. Further elaboration on the data used in this study is provided in [10] detailing the increasing trend of insect radar echoes detected before and during the infestation period. It is important to note that FAW are nocturnal insects, while most birds in tropical regions, including Rwanda, are active during the day and at the end of the day. Nocturnal bird species like owls and nightjars are not abundant in this region.

FAW ground reports were collected by farmers from three districts in the southern province (Nyanza, Huye, and Gisagara) to assess the distance between the radar and the FAW infestation reports. Figure 1 includes a map of Rwanda, highlighting the radar site and the districts reporting FAW infestations. The distances from the radar to Nyanza, Huye, and Gisagara Districts are within approximately 25 km and 95 km. Bold black lines in the right panel indicate the distance and height from the radar to the study area and the elevation angles used, considering the height or insect flight layer.

Figure 1 also outlines Meteo Rwanda's scanning strategy, showing that the radar beam points toward the infested areas. The beam height ranges from 200 m to 2000 m for the first three elevation angles (0.5, 1.5, and 2.5 degrees). This range encompasses the typical flight altitudes of migratory insects, which usually fly between 150 and 1200 m above ground level [34,35]. Additionally, the figure demonstrates that the beam profile is not obstructed by ground clutter, as evidenced by a clear air beam profile for a beam pointed at 225 degrees toward the Nyanza and Huye Districts.

Insect migration predominantly occurs at high altitudes, often hundreds of meters above the ground, where insects utilize strong winds to travel quickly and cover long distances. The majority of these migrations take place between 150 and 1200 m above ground level, with medium-sized insects, weighing between 10 and 70 mg, being the most common travelers. These insects include species like butterflies, dragonflies, and moths [36].

2.3. Derivation of the Depolarization Ratio (DR)

The Meteo Rwanda C-band dual-polarization weather radar currently lacks automatic calculation of the DR parameter, unlike other basic dual-polarization parameters. To address this, we utilized the bioRad R package (version 0.7.0.9603) [37], which offers tools for accessing, visualizing, and analyzing weather radar data for biological studies. In line with methodologies detailed in [37], we used the calculate_param() function within the bioRad package to compute and integrate the DR parameter using expressions outlined in previous studies. This computation was conducted within the Meteo Rwanda radar's TITAN software environment [30], facilitating easy access to radar data and updates following DR derivation. For a comprehensive understanding of the computation process, refer to the accompanying flowchart (Figure 2), which provides insight into the derivation of DR.

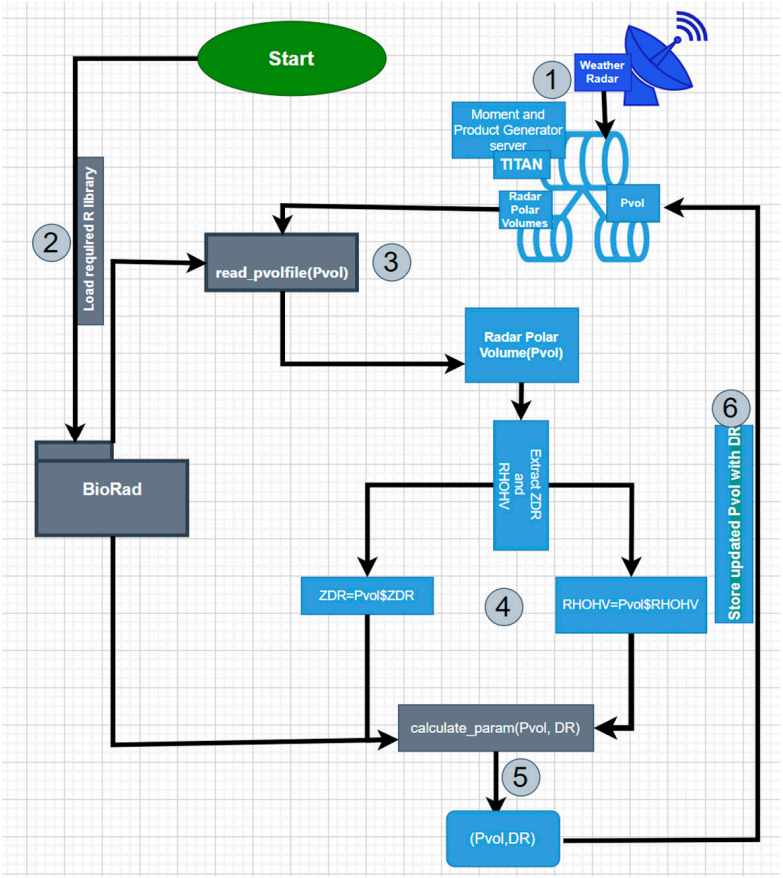

Figure 2. Flowchart for Depolarization Ratio (DR) derivation and integration into the TITAN system.

DR proves particularly beneficial for airborne targets like insects and birds [11]. Unlike rain or hail, the biometeors exhibit erratic movements and rapid changes in orientation while flying. Such dynamic behavior significantly impacts the polarization of the incident radar signal. By incorporating DR into radar analysis, meteorologists gain a deeper understanding of how these dynamic targets interact with radar waves [11,38]. This enhanced understanding translates to more accurate classification and identification, not just for weather phenomena, but also for scenarios where biometeors might be present. The ability to distinguish between these targets becomes crucial for various applications, from aviation safety to improving the accuracy of weather forecasts.

As established by various researchers [12,22,24,28,38], the DR is mathematically expressed as follows [5]:

$$DR = 10\, log_{10} \frac{\left(\mathrm{ZDR} + 1 - 2 * \sqrt{\mathrm{ZDR}} * \mathrm{RHOHV}\right)}{\left(\mathrm{ZDR} + 1 + 2 * \sqrt{\mathrm{ZDR}} * \mathrm{RHOHV}\right)} \quad (1)$$

where:

ZDR: Logarithmic ratio of horizontal to vertical reflectivity.

RHOHV: Measures the similarity in polarization between transmitted and received signals.

Sqrt(ZDR): Represents the magnitude of depolarization caused by the scatters.

In our study, this equation is implemented utilizing the existing measurements of ZDR and RHOHV to estimate DR. This approach eliminates the need for a dedicated LDR measurement mode [11], making DR a practical and valuable tool for dual-polarization weather with simultaneous transmission and reception weather radar systems like the one operated by Meteo Rwanda.

Figure 2 depicts the process of calculating and integrating the DR into the Meteo Rwanda weather radar system. The derivation process is classified into six key steps, as shown in the figure:

1. Accessing Radar: Every 5 min, weather radar polar data volumes are received, processed, and stored by the Moment and Product Generator (MGEN/PGEN) within the TITAN environment where real-time data are accessed.
2. R Package and Library Loading: Required package and library are loaded following the methodology proposed by Kilambi et al. (2018) [11] and also using the bioRad R package (version 0.7.0.9603) developed by Dokter (Dokter et al., 2019) [37].
3. Reading Polar Volume Data: We work with low-level radar data, known as polar volume data, which the bioRad package interacts with. The package reads polar volumes using the read_pvolfile function, returning the volume as a pvol object (Dokter et al., 2019) [37].
4. Extracting ZDR and RHOHV: From the "pvol" object obtained in step 3, we extract the differential reflectivity (ZDR) and copolar correlation coefficient (RHOHV), which are crucial parameters from dual-polarization radar systems.
5. DR Calculation: Using the calculate_param function on the pvol object, we compute DR as a new parameter. This calculation utilizes the ZDR and RHOHVvalues extracted in step 4 and follows Equation (1).
6. DR Integration and Storage: The calculated DR parameters are then stored within the pvol object, effectively updating the radar data. The updated data, including the newly integrated DR, are subsequently stored in the Product Generation server (PGEN).

This integration process allows for the real-time derivation and archiving of DR alongside other weather radar parameters.

2.4. The DR Signature for Airborne Biological Targets

Airborne biological targets such as insects and birds have irregular shapes and varying orientations, leading to significant depolarization effects. Due to their irregular shapes, biological targets tend to exhibit larger absolute values of ZDR (|ZDR|) compared to hydrometeors which are more spherical in shape and typically have similar reflectivity in both horizontal and vertical polarization. The depolarization term, represented by |ZDR|, dominates the numerator in the DR Equation (1) for biological targets. As a result, the DR values for biological targets are typically significantly different than those for hydrometeors.

However, weather echoes with higher depolarization, such as those from hail and possibly melting graupel, are exceptions. As we are focusing on clear air events, these exceptions are not included. Since hail generally is not observed during clear air periods and has reflectivities never seen in biological echoes (>35 dBZ), applying a reflectivity

threshold helps recognize them as weather. This filtering out of weather particles enhances data cleaning and preparation.

Insect Targets:

For insect targets, which exhibit significant depolarization due to their irregular shapes, we expect | ZDRinsect | to be high >1, and low values of RHOHVinsect < 0.88) indicate less similarity in polarization between transmitted and received signal,

$$\text{DRinsect} = 10\log_{10}\frac{\text{ZDRinsect} + 1 - 2 * \sqrt{\text{ZDRinsect}} * \text{RHOHVinsect}}{\text{ZDRinsect} + 1 + 2 * \sqrt{\text{ZDRinsect}} * \text{RHOHVinsect}} \quad (2)$$

2.5. Integrating Depolarization Ratio (DR) in Fuzzy Logic

The precision of weather radar target classification can be greatly improved by incorporating multiple parameters. For example, the research by Wang et al. [13] demonstrates that a comprehensive use of polarimetric measurements derived from dual-polarization Doppler weather radar data enhances the accuracy of identifying various types of hydrometeors. Differences in the shape, size, and spatial orientation of different hydrometeors generate distinct polarization parameters, which can significantly advance hydro meteorological classification using these polarization measurements.

To tackle these challenges, integrating Depolarization Ratio (DR) into fuzzy logic weather radar data classification is pivotal. This integration enhances the ability to accurately discern and classify biological targets, especially given their dynamic flight nature. The objective is to advance the accuracy of target identification and classification in weather radar applications, with a specific focus on FAW detection and identification.

The simplified proposed fuzzy logic integrating DR (FL_DR) is illustrated in Figure 3 below:

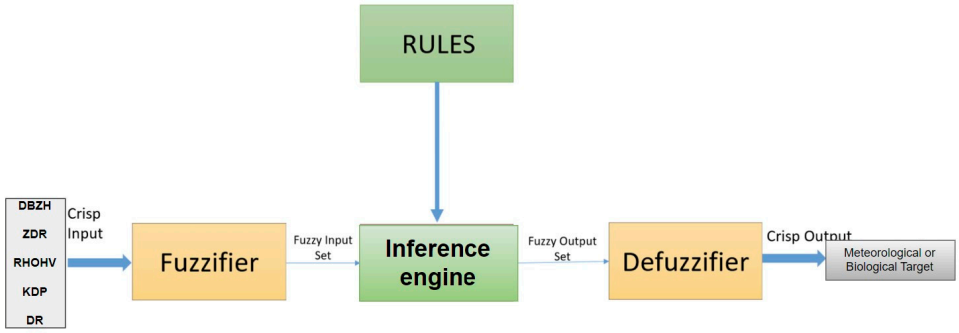

Figure 3. A simplified fuzzy logic architecture comprising four key components and utilizing five crisp inputs (DBZH, ZDR, RHOHV, KDP, and DR) for the classification of weather radar echoes in Rwanda as either meteorological or biological.

The FL_DR classification method is used to classify radar pixels into either a meteorological or biological category, relying on predefined membership rules [10]. This method builds upon a previous research study [10], which was adopted following a method proposed by [26] using fuzzy logic to class hydrometeors.

Essentially, each radar pixel is classified based on a set of its values for parameters including DBZH, ZDR, KDP, RHOHV, and DR. If all of these parameter values fall within the range of a single class, the pixel is straightforwardly classified into that class. However, when there are overlaps in parameter values, classification is still possible. In this case, the membership degree to which each pixel belongs to a particular class can vary. This means that while some parameters might lean towards one class, others might lean towards the other. In such cases, the determination of a pixel's class hinges on the collective degree of membership across all parameters. This collective membership degree serves as the deciding factor.

Yet, there are scenarios where there is no overlap in one or more parameters. In these instances, the dominant class is determined not only by the presence of membership but also by the number of membership degrees. This approach allows FL and FL_DR for a flexible and nuanced classification process that accounts for the varying degrees of certainty in categorizing radar pixels.

3. Results and Discussion

Understanding the pairwise relationship between ZDR and RHOHV is pivotal as they discern meteorological from non-meteorological targets, underlining the importance of target density analysis. The derivation of the Depolarization Ratio from these metrics notably enhances target classification precision, as evidenced by prior studies [11,22].

Figure 4 provides a detailed exploration of both biological and meteorological targets within the ZDR-RHOHV space, leveraging our comprehensive training dataset consisting of 1,308,956 nocturnal clear air radar echo pixels. On the left side of Figure 4, we delve into the density of biological targets, predominantly represented by Fall Armyworm (FAW). Here, we observe 850,821 clear air radar echoes categorized as biological targets, along with 458,135 echoes classified as meteorological targets. Conversely, the right side of Figure 4 focuses on the density of meteorological targets, based on 458,135 clear air radar echoes.

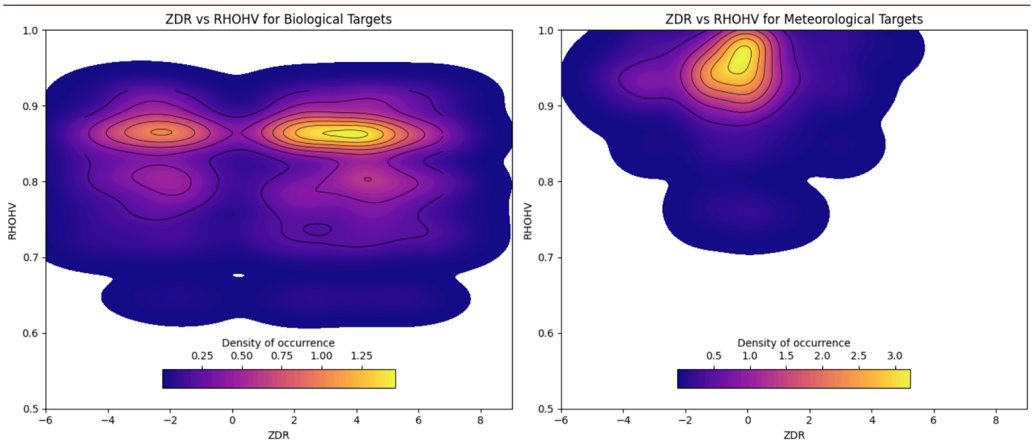

Figure 4. Spatial distribution of biological and meteorological targets in the ZDR-RHOHV Space.

The contour lines within the plot delineate areas of equal probability density, shedding light on variations in the density of biological targets (insects) or meteorological targets (weather phenomena) across the ZDR-RHOHV space. Thicker contour lines highlight regions of higher density, while thinner lines indicate areas of lower density. This visualization aids in understanding the spatial distribution of targets, enabling the identification of prevalent target categories for specific ZDR-RHOHV value pairs.

Specifically, for biological targets, higher densities are observed within the ZDR range of −6 dB to +6 dB and RHOHV range of 0.68 to 0.91. Notably, the highest density regions occur between −4 dB to −2 dB and +2 dB to +6 dB for ZDR, and 0.8 to 0.9 for RHOHV. Conversely, for meteorological targets, the highest density regions are typically observed near ZDR values close to 0 dB and RHOHV values greater than 0.9.

3.1. Implementation of Depolarization Ratio (DR) Derivation

Since the Meteo Rwanda C-band Doppler polarimetric weather radar does not automatically compute DR, we derived it directly from the radar data using the parameters of differential reflectivity and correlation coefficient. Following the methodology and procedural steps outlined in the flow chart shown in Figure 2, we obtained DR. To illustrate this process, we present an example demonstrating the computed DR for a clear air event on 12 November 2020, at 5:20:11 (Kigali Time, UCT+2).

Figure 5 depicts data from a clear air event on 12 November 2020, at 5:20:11 a.m. (Kigali, Time, UCT+2), showing Differential Reflectivity and Correlation Coefficient alongside the newly derived DR. This observation, conducted at a 0.5-degree elevation angle amidst the FAW outbreak in maize fields, reveals that insect signatures typically exhibit DR values exceeding −13 dB, ZDR values between 2 dB and 7 dB, reflectivity (DBZH) under 30 dBZ, and a correlation coefficient (RHOHV) below 0.88, often associated with biological phenomena. Evaluating the FL_DR algorithm's accuracy compared to the standard FL involves analyzing on-site observations of adult FAW moths in maize fields. This includes examining the classification output of radar echoes produced by both FL_DR and FL algorithms, applied to radar data collected over infested maize areas and maize marshlands during FAW outbreaks spanning from September 2020 to January 2021.

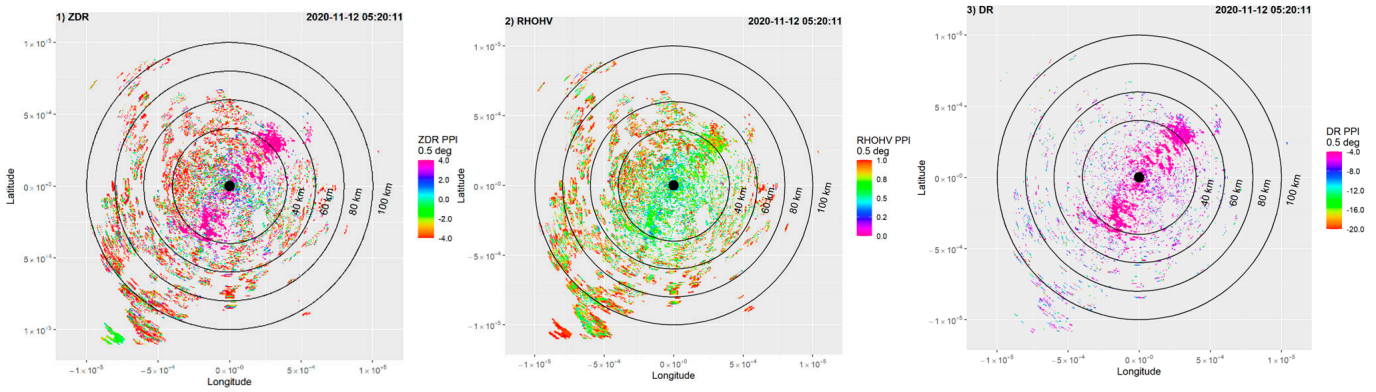

Figure 5. Meteo Rwanda Radar captured a clear air event on 12 November 2020, at 5:20 a.m., displaying ZDR, RHOHV, and DR during a FAW outbreak.

3.2. Integrating DR in Fuzzy Logic (FL_DR)

Clear Air Event Case for FAW Radar Echoes Detection on 12 November 2020

Our research aimed to improve the detection of airborne biological particles, focusing specifically on FAW outbreaks between October 2020 and January 2021. We sought to enhance existing fuzzy logic (FL) systems by integrating DR, a polarimetric radar parameter. We used the TITAN\lrose software (lrose-core-20240525) from Meteo Rwanda to visualize and gain more insight of the output of a standard FL system and an upgraded version that incorporated DR alongside additional parameters (FL_DR).

The data in Figure 6 (upper panel) demonstrate that the FL_DR algorithm outperforms FL in detection capabilities, particularly beyond a 50 km range from the radar site, attributed to consideration of depolarization effects from the target. Within a 50 km radius, both algorithms perform similarly, as observed over maize fields around the Akanyaru River in Gisagara and Nyanza districts. However, beyond this range, FL_DR excels in detecting biological echoes at significant distances, highlighting its potential for improving the monitoring of airborne agricultural pests. The lower panel shows corresponding ZDR and RHOHV values; when FL and FL_DR algorithms detect more insects, it corresponds with ZDR values between 2 and 7 dB and RHOHV values between 0.7 and 0.88, typical for insect signatures. However, due to the tropical weather and climate in Rwanda, it is common to encounter hydrometeors in the sky, often caused by cloud formations such as stratocumulus and altocumulus clouds. These clouds form when a layer of air is lifted and cooled, often by a weak frontal system, and usually indicate stable weather but can bring drizzle [39]. Under these weather conditions, insects can fly, which explains why Figure 6 shows the possibility of seeing weather particle echoes. This is naturally related to the tropical weather conditions.

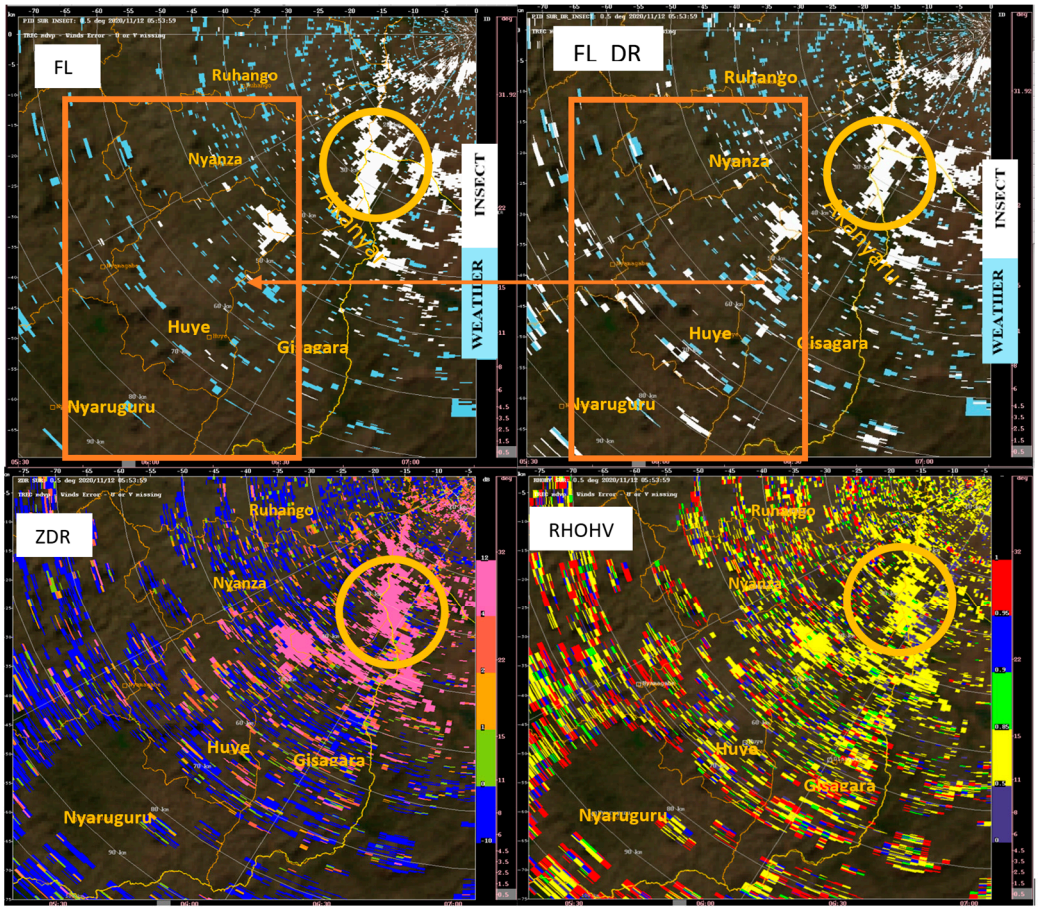

Figure 6. Comparison of FL and FL_DR weather radar detecting FAW adult moths, an example of 12 November 2020, 20–40 min before sunrise. Lower panels show differential reflectivity (**left**) and correlation coefficient (**right**). The circled area highlights concentrated insect echoes indicating detected insect activity. The orange boxes illustrate the enhanced insect detection capability of FL_DR compared to FL.

4. Performance Evaluation

A comparative assessment was conducted between a novel fuzzy logic algorithm incorporating Depolarization Ratio (FL_DR) and the standard fuzzy logic (FL), which utilizes only four standard polarimetric parameters. The training dataset consisted of 1,308,956 radar echo pixels collected from 18 October 2020 to 29 November 2020, covering both nocturnal clear air and non-clear air events. The analysis compared the results of our previous study [10], where FL was applied to the same data, with the results of FL_DR, which incorporate DR.

Both FL and FL_DR classify radar pixels as either meteorological or biological targets based on specific logic and rules. If all parameter values (DBZH, ZDR, KDP, RHOHV, and DR) belong to one class, the classification is straightforward. However, overlaps exist where parameter values have varying degrees of membership in each class. In cases where values overlap across all parameters, the membership degree determines the pixel's classification. If there is overlap in one or more parameters, the dominant class is determined by the number of membership degrees. This method offers flexibility in accounting for uncertainties in classifying radar pixels.

For the testing dataset, comprising 1,045,102 weather radar nocturnal echo pixels sampled during clear air events amidst a Fall Armyworm outbreak in the Nyanza, Huye, and Gisagara Districts from 30 November 2020 to January 2021, over maize fields and

marshland, FL with four parameters and FL_DR with five input parameters, including DR, were trained and tested on these samples.

The resulting classification outputs were compared using the Fraction of Echoes Correctly Identified (FEI) and Heidke Skill Score (HSS). FEI measures accuracy as a percentage, while HSS assesses the algorithm's skill, with values ranging from −1 to 1, where 1 signifies perfect skill and 0 indicates no skill or random performance. Table 1 presents the comparative performance analysis of FL_DR against FL.

$$FEI = \frac{NC * 100}{T} \tag{3}$$

While the Heidke Skill Score (HSS) is given by:

$$HSS = \frac{\mathrm{NC} - (C_{12} * C_{21}/\mathrm{T})}{\mathrm{T} - (C_{12} * C_{21}/\mathrm{T})} \tag{4}$$

- NC is the number of correctly identified echoes.
- T is the total number of classifications attempted.
- C_{12} is the number of cases where a meteorological echo was incorrectly classified as a biological echo.
- C_{21} is the number of cases where a biological echo was incorrectly classified as a meteorological echo.

Table 1. The performance metrics of Fuzzy Logic (FL) and Fuzzy Logic with Depolarization Ratio (FL_DR) for identifying meteorological targets (M.T) and biological targets (B.T), and a comparison with similar work by Kilambi et al. (2018) using the DR threshold method.

Performance Metrics	FL [11]		FL_DR		Kilambi et al. [11]			
	DR > −13 dB				DR > −12 dB		With RHOHV and ZDR	
	M.T	B.T	M.T	B.T	M.T	B.T	M.T	B.T
FEI	87.02%	98.42%	95.81%	98.93%	97.1%	95.8%	95.1%	97.4%
HSS	0.98	0.98	0.96	0.98	0.93	0.97	0.89	
Hits	336,398	611,506	359,707	662,480	-	-	-	-
Misses	39,038	58,160	15,729	7186	-	-	-	-
False Alarm	58,160	39,038	7186	15,729	-	-	-	-

Table 1 compares the performance metrics of three methods: Fuzzy Logic (FL), Fuzzy Logic with Depolarization Ratio (DR) integration (FL_DR), and a threshold method by Kilambi et al. [11]. The analysis shows significant improvements in identifying biological and meteorological targets from weather radar data using FL_DR. This method enhances the Fraction of Echoes Correctly Identified (FEI), achieving 95.81% accuracy for weather and 98.93% for non-weather targets, surpassing conventional FL. Additionally, the Heidke Skill Score (HSS) supports FL_DR's superior performance, with scores of 0.96 for weather and 0.98 for non-weather echoes, indicating high proficiency in distinguishing between event types.

Figure 7 presents a comparative analysis of confusion matrices for FL and FL_DR during the Fall Armyworm (FAW) outbreak from October 2020 to January 2021 in the Nyanza, Huye, and Gisagara Districts. The integration of DR in FL_DR led to significant improvements in classification accuracy. For meteorological radar echoes, FL_DR increased classification accuracy from 87.02% to 95.81%, reducing incorrect classifications from 12.98% to 4.19%. For biological targets, classification accuracy increased from 98% to 98.93%, with incorrect classifications decreasing from 1.58% to 1.07%. Notably, FL_DR demonstrated lower false positive rates compared to FL. The DR threshold method for

biological and meteorological targets at DR > −12 dB showed an FEI of 97.1% and an HSS of 0.9257 for meteorological targets, and an FEI of 95.8% and an HSS of 0.8939 for biological targets.The integration of Depolarization Ratio (DR) into fuzzy logic significantly enhances precision, reliability, and overall performance in radar-based target identification for both weather and non-weather events. This improvement highlights the effectiveness of FL_DR in distinguishing between meteorological and biological echoes, especially during events such as the FAW outbreak. The strong correlation observed between radar predictions and ground observations further solidifies FL_DR as a robust tool for accurately identifying and classifying various types of radar echoes, thereby aiding in effective decision-making processes.

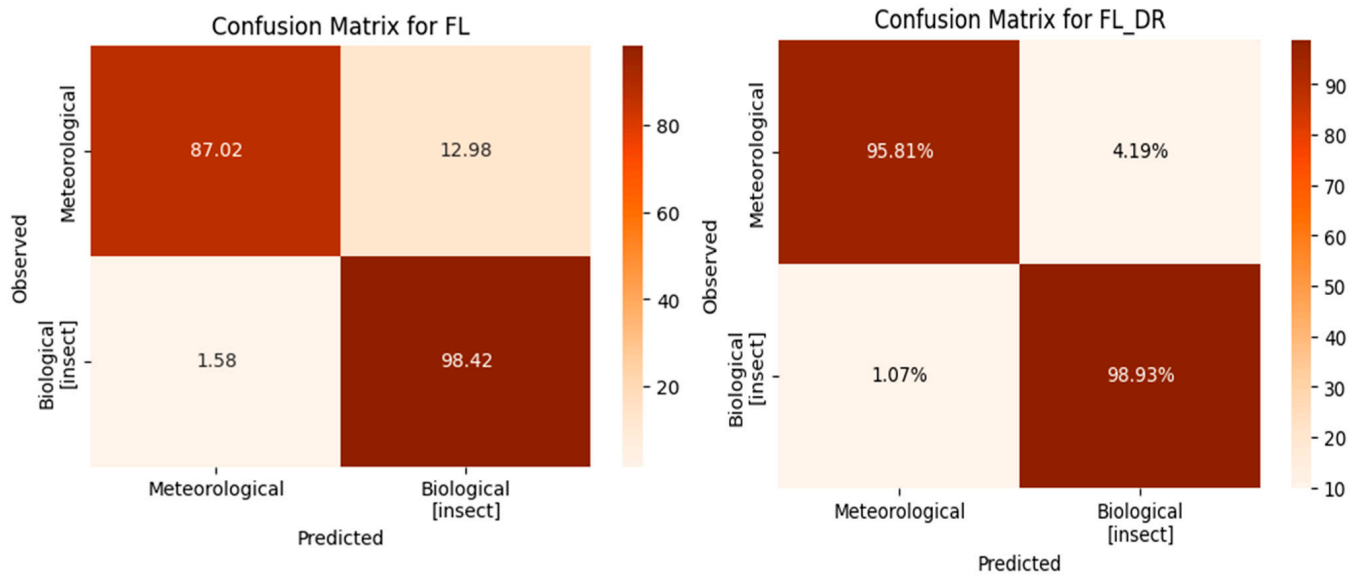

Figure 7. Confusion matrices depicting the alignment between radar-based target identification using Fuzzy Logic (FL) and Fuzzy Logic integrated with Depolarization Ratio (FL_DR), validated against Fall Armyworm outbreak observations data and a heavy rain event.

To refine our performance evaluation, we conducted a comprehensive Precision–Recall (PR) analysis, using PR curves and associated Area Under the Curve (AUC-PR) values to assess the effectiveness of our proposed fuzzy logic algorithm, FL_DR, compared to FL. The PR curve demonstrates the balance between precision (correctly identified positive cases) and recall (true positive cases correctly identified) for different classification thresholds. A higher AUC-PR value indicates better overall performance. Our focus was on detecting and classifying meteorological (weather) and biological (insect) radar echoes (see Figure 8). For this analysis, we utilized the Python programming language and the sci-kit-learn library, employing the precision_recall_curve and average_precision_score functions from the sklearn metrics module to compute the PR curve and AUC-PR for each classification output from FL_DR and FL. The curves in Figure 8 illustrate the precision–recall performance of FL_DR compared to FL, showcasing their ability to distinguish between weather and insect radar echoes. Higher AUC-PR values indicate superior performance in both precision and recall.

Our analysis drew from a dataset of 1,045,102 weather radar echo pixels comprising 843,237 nocturnal clear air radar echoes extracted over FAW-infested fields and maize marshlands. These radar echo pixels were collected and extracted from 30 random points (location with infested maize fields and marshland) across Nyanza, Gisagara, and Huye Districts during September and October 2020, covering altitudes ranging from 200 m to 2000 m, with a 200 m sampling vertical resolution.

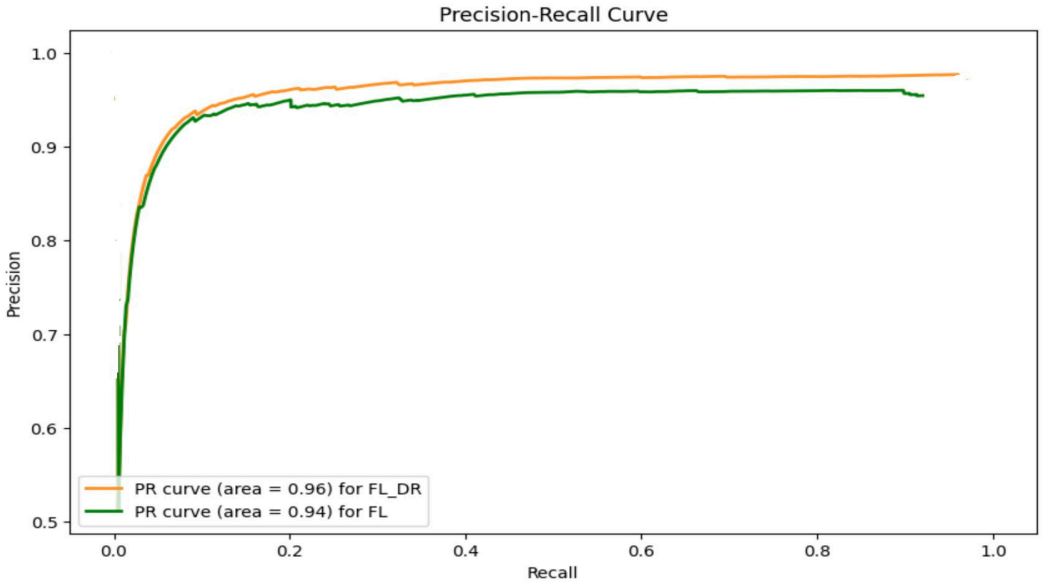

Figure 8. Precision–Recall analysis of FL_DR and FL for meteorological and biological radar echoes detection and classification.

In this comparison, the PR curve for FL_DR showcased a marginally larger Area Under the Curve (AUC) of 0.96 compared to FL, which achieved an AUC of 0.94. These notable AUC-PR values indicate good performance in distinguishing between weather (meteorological) and biological (insect) radar echoes. AUC-PR values nearing 1 demonstrate high precision and recall across various threshold values, highlighting the fuzzy logic algorithm's proficiency in achieving both a low false positive rate and a low false negative rate.

Moreover, these results underscore the remarkable performance of both classifiers in distinguishing between weather and insect radar echoes, with FL_DR demonstrating a slight advantage over FL based on the AUC-PR values. It is essential to highlight the significance of FL_DR's capability to leverage DR data alongside other radar variables and consider integrating depolarization effects from radar targets, especially bio meteors, which often exhibit changing directions and positions, unlike weather targets.

5. Conclusions

The challenge of distinguishing insect swarms from weather patterns poses a significant obstacle to the effective utilization of weather radar applications. Our study addresses this challenge by leveraging Meteo Rwanda's weather radar data collected during a FAW outbreak and infestation of maize crop fields in three districts of Rwanda's southern province from September 2020 to January 2021.

We adopted a method that analyzes ZDR and RHOHV to estimate DR, a crucial parameter for understanding how objects modify radar signals. While existing metrics provide valuable insights, they also possess limitations. To overcome these limitations, we developed FL_DR, an advanced fuzzy logic algorithm integrating DR. Our findings demonstrate that FL_DR significantly enhances accuracy in identifying both insects (from 98.42% to 98.93%) and weather phenomena (from 87.03% to 95.82%) compared to a standard FL algorithm. This enhanced detection capability positions FL_DR as a valuable system for monitoring, identification, and warning of environmental phenomena in regions similar to tropical areas facing FAW outbreaks. Additionally, it could be tested and further refined for other migrating biological targets such as birds, insects, or bats.

In future research, it would be essential to explore the integration of advanced techniques such as aerial light traps and camera drones to enhance validation and refinement processes. These methodologies offer significant promise in providing real-time sampling of bio-scatters from the atmosphere, allowing for correlation with radar-detected echoes.

Additionally, there is considerable potential in incorporating DR into other machine learning algorithms, such as Random Forest, XGBoost, and SVM, to improve the identification of hydrometeors and diverse airborne biological targets.

Author Contributions: Conceptualization, F.M. and A.V.; Methodology, F.M., A.V., K.S.K., G.R. and E.N.; Software, F.M.; Formal analysis, F.M. and A.V.; Resources, F.M., A.V. and K.S.K.; Data curation, F.M.; Writing—original draft, F.M. and A.V.; Writing—review and editing, A.V., K.S.K., G.R. and E.N. All authors have read and agreed to the published version of the manuscript.

Funding: This research received no external funding.

Data Availability Statement: The data supporting the findings of this study can be obtained from the corresponding author upon reasonable request.

Acknowledgments: This research was made possible through the collaborative efforts of the African Center of Excellence in Internet of Things (ACEIoT) at the University of Rwanda's College of Science and Technology the Partnership for Skills in Applied Sciences, Engineering, and Technology (PASET) through the Regional Scholarship and Innovation Fund (RSIF), The Seoul National University (SNU), and the National Council for Science and Technology (NCST) through a Research and Innovation Mobility Grant (RIM), We are also grateful to the Rwanda Meteorology Agency for their invaluable contribution by providing access to their weather radar.

Conflicts of Interest: The authors declare no conflicts of interest.

References

1. Maino, J.L.; Schouten, R.; Overton, K.; Day, R.; Ekesi, S.; Bett, B.; Barton, M.; Gregg, P.C.; Umina, P.A.; Reynolds, O.L. Regional and seasonal activity predictions for fall armyworm in Australia. *Curr. Res. Insect Sci.* **2021**, *1*, 100010. [CrossRef] [PubMed]
2. Florio, J.; Verú, L.; Dao, A.; Yaro, A.S.; Diallo, M.; Sanogo, Z.L.; Samaké, D.; Huestis, D.L.; Yossi, O.; Talamas, E.; et al. Massive windborne migration of Sahelian insects: Diversity, seasonality, altitude, and direction. *bioRxiv* **2020**, 1–32. [CrossRef]
3. One Acre Fund. Responding to Fall Armyworm Outbreaks in Africa. 2019. Available online: https://oneacrefund.org/blog/responding-fall-armyworm-outbreaks-africa/1%E2%80%9313 (accessed on 25 May 2021).
4. Westbrook, J.K.; Eyster, R.S.; Wolf, W.W. WSR-88D doppler radar detection of corn earworm moth migration. *Int. J. Biometeorol.* **2014**, *58*, 931–940. [CrossRef] [PubMed]
5. Tang, L.; Zhang, J.; Wang, Y.; Howard, K.W. Identification of biological and anomalous propagation echoes in weather radar observations—An imaging processing approach. In Proceedings of the 35th Conference on Radar Meteorology, Williamsburg, VA, USA, 26–30 September 2011; p. 11.123.
6. Goergen, G.; Kumar, P.L.; Sankung, S.B.; Togola, A.; Tamò, M. First report of outbreaks of the fall armyworm spodoptera frugiperda (J E Smith) (Lepidoptera, Noctuidae), a new alien invasive pest in West and Central Africa. *PLoS ONE* **2016**, *11*, e0165632. [CrossRef] [PubMed]
7. Abrahams, P.; Bateman, M.; Beale, T.; Clottey, V.; Cock, M.; Colmenarez, Y.; Corniani, N.; Early, R.; Godwin, J.; Gomez, J.; et al. Fall Armyworm: Impacts and Implications for Africa. *Outlooks Pest Manag.* **2017**, *5*, 196–201.
8. Uzayisenga, B.; Waweru, B.; Kajuga, J.; Karangwa, P.; Uwumukiza, B.; Edgington, S.; Thompson, E.; Offord, L.; Cafá, G.; Buddie, A. First Record of the Fall Armyworm, *Spodoptera frugiperda* (J.E. Smith, 1797) (Lepidoptera: Noctuidae), in Rwanda. *Afr. Entomol.* **2018**, *26*, 244–246. [CrossRef]
9. Abrahams, O. *Fall Armyworm: Impacts and Implications for Africa*; Evidence Note; CABI: Wallingford, UK, 2018; p. 144.
10. Maniraguha, F.; Vodacek, A.; Kim, K.S.; Ndashimye, E.; Rushingabigwi, G. Adopting a Neuro-Fuzzy Logic Method for Fall Armyworm Detection and Monitoring Using C-Band Polarimetric Doppler Weather Radar with Field Verification. *IEEE Trans. Geosci. Remote Sens.* **2024**, *62*, 5105910. [CrossRef]
11. Kilambi, A.; Fabry, F.; Meunier, V. A simple and effective method for separating meteorological from nonmeteorological targets using dual-polarization data. *J. Atmos. Ocean. Technol.* **2018**, *35*, 1415–1424. [CrossRef]
12. Radhakrishna, B.; Fabry, F.; Kilambi, A. Fuzzy logic algorithms to identify birds, precipitation, and ground clutter in S-band radar data using polarimetric and nonpolarimetric variables. *J. Atmos. Ocean. Technol.* **2019**, *36*, 2401–2414. [CrossRef]
13. Wang, H.; Ran, Y.; Deng, Y.; Wang, X. Study on deep-learning-based identification of hydrometeors observed by dual polarization Doppler weather radars. *Eurasip J. Wirel. Commun. Netw.* **2017**, *2017*, 173. [CrossRef]
14. Melnikov, V.M.; Istok, M.J.; Westbrook, J.K. Asymmetric radar echo patterns from insects. *J. Atmos. Ocean. Technol.* **2015**, *32*, 659–674. [CrossRef]
15. Jatau, P.; Melnikov, V.; Yu, T.-Y. Detecting Birds and Insects in the Atmosphere Using Machine Learning on NEXRAD Radar Echoes. *Environ. Sci. Proc.* **2021**, *8*, 48. [CrossRef]
16. Manoj, E.; Sharma, K.; Kumar, M. A Survey in fuzzy Logic: An Introduction. *IJSRD-Int. J. Sci. Res. Dev.* **2015**, *3*, 822–824.

17. Marzano, F.S.; Scaranari, D.; Montopoli, M.; Vulpiani, G. Supervised classification and estimation of hydrometeors from C-band dual-polarized radars: A Bayesian approach. *IEEE Trans. Geosci. Remote. Sens.* **2008**, *46*, 85–98. [CrossRef]
18. Jatau, P.; Melnikov, V. Classifying Bird and Insect Radar Echoes At S-Band. In Proceedings of the 35th Conference on Environmental Information Processing Technologies, Phoenix, AZ, USA, 6–10 January 2019; p. 830.
19. Kessinger, C.; Ellis, S. The radar echo classifier: A fuzzy logic algorithm for the WSR-88D. In Proceedings of the 3rd Conference on Artificial Intelligence Applications to the Environmental Science, Perth, Australia, 3–5 December 2003; pp. 1–11.
20. Rojas, D.; Zambrano, C.; Varas, M.; Urrutia, A. A multi-level thresholding-based method to learn fuzzy membership functions from data warehouse. In Proceedings of the Pattern Recognition, Image Analysis, Computer Vision, and Applications: 16th Iberoamerican Congress, CIARP 2011, Pucón, Chile, 15–18 November 2011; pp. 664–674. [CrossRef]
21. Park, H.S.; Ryzhkov, A.V.; Zrnić, D.S.; Kim, K.E. The hydrometeor classification algorithm for the polarimetric WSR-88D: Description and application to an MCS. *Weather Forecast.* **2009**, *24*, 730–748. [CrossRef]
22. Ryzhkov, A.; Matrosov, S.Y.; Melnikov, V.; Zrnic, D.; Zhang, P.; Cao, Q.; Knight, M.; Simmer, C.; Troemel, S. Estimation of depolarization ratio using weather radars with simultaneous transmission/reception. *J. Appl. Meteorol. Clim.* **2017**, *56*, 1797–1816. [CrossRef]
23. Myagkov, A.; Seifert, P.; Bauer-Pfundstein, M.; Wandinger, U. Cloud radar with hybrid mode towards estimation of shape and orientation of ice crystals. *Atmos. Meas. Tech.* **2016**, *9*, 469–489. [CrossRef]
24. Matrosov, S.Y. Depolarization estimates from linear H and V measurements with weather radars operating in simultaneous transmission-simultaneous receiving mode. *J. Atmos. Ocean. Technol.* **2004**, *21*, 574–583. [CrossRef]
25. Ryzhkov, A.; Zhang, P.; Cao, Q.; Matrosov, S.; Melnikov, V.; Knight, M. Measurements of Circular Depolarization Ratio with the Radar with Simultaneous Transmission/Reception. In Proceedings of the Extended Abstracts, Eighth European Conf. on Radar in Meteorology and Hydrology, Garmisch-Partenkirchen, Germany, 1–5 September 2014; pp. 1–10.
26. Liu, H.; Chandrasekar, V. Classification of hydrometeors based on polarimetric radar measurements: Development of fuzzy logic and neuro-fuzzy systems, and in situ verification. *J. Atmos. Ocean. Technol.* **2000**, *17*, 140–164. [CrossRef]
27. Williams, C.R.; Johnson, K.L.; Giangrande, S.E.; Hardin, J.C.; Öktem, R.; Romps, D.M. Identifying insects, clouds, and precipitation using vertically pointing polarimetric radar Doppler velocity spectra. *Atmos. Meas. Tech.* **2021**, *14*, 4425–4444. [CrossRef]
28. Overeem, A.; Uijlenhoet, R.; Leijnse, H. Full-year evaluation of nonmeteorological Echo removal with dual-polarization fuzzy logic for two C-band radars in a temperate climate. *J. Atmos. Ocean. Technol.* **2020**, *37*, 1643–1660. [CrossRef]
29. Maniraguha, F.; Vodacek, A.; Ndashimye, E.; Rushingabigwi, G. Ground Clutter Mitigation and Insect Signature Detection for Polarimetric C-Band Doppler Weather Radar. In Proceedings of the 2021 11th IEEE Global Humanitarian Technology Conference GHTC, Seattle, WA, USA, 19–23 October 2021; pp. 289–296. [CrossRef]
30. Michael Dixon, G.W. TITAN: Thunderstorm Identification, Tracking, Analysis, and Nowcasting—A Radar-based Methodology. *J. Atmos. Ocean. Technol.* **1993**, *10*, 785–797. [CrossRef]
31. He, S.; Wang, L.; Zhu, D.; Qian, J. Thunderstorm identification method research for airborne weather radar. In Proceedings of the International Conference on Signal Processing and Communication Technology (SPCT 2021), Online, 25 December 2021; 12178p. [CrossRef]
32. Brandt, M.J.; Cresswell, W. Diurnal foraging routines in a tropical bird, the rock finch Lagonosticta sanguinodorsalis: How important is predation risk? *J. Avian Biol.* **2009**, *40*, 90–94. [CrossRef]
33. Mallon, J.M.; Tucker, M.A.; Beard, A.; Bierregaard, R.O.; Bildstein, K.L.; Böhning-Gaese, K.; Brzorad, J.N.; Buechley, E.R.; Bustamante, J.; Carrapato, C.; et al. Diurnal timing of nonmigratory movement by birds: The importance of foraging spatial scales. *J. Avian Biol.* **2020**, *51*, 2612. [CrossRef]
34. Kimura, M.T. Altitudinal migration of insects. *Entomol. Sci.* **2021**, *24*, 35–47. [CrossRef]
35. Atieli, H.E.; Zhou, G.; Zhong, D.; Wang, X.; Lee, M.-C.; Yaro, A.S.; Diallo, M.; Githure, J.; Kazura, J.; Lehmann, T.; et al. Wind-assisted high-altitude dispersal of mosquitoes and other insects in East Africa. *J. Med. Entomol.* **2023**, *60*, 698–707. [CrossRef] [PubMed]
36. Hu, G.; Lim, K.S.; Reynolds, D.R.; Reynolds, A.M.; Chapman, J.W. Wind-related orientation patterns in diurnal, crepuscular and nocturnal high-altitude insect migrants. *Front. Behav. Neurosci.* **2016**, *10*, 32. [CrossRef] [PubMed]
37. Dokter, A.M.; Desmet, P.; Spaaks, J.H.; van Hoey, S.; Veen, L.; Verlinden, L.; Nilsson, C.; Haase, G.; Leijnse, H.; Farnsworth, A.; et al. bioRad: Biological analysis and visualization of weather radar data. *Ecography* **2019**, *42*, 852–860. [CrossRef]
38. Matrosov, S.Y. Evaluations of the spheroidal particle model for describing cloud radar depolarization ratios of ice hydrometeors. *J. Atmos. Ocean. Technol.* **2015**, *32*, 865–879. [CrossRef]
39. Wood, R. Clouds and Fog: Stratus and Stratocumulus. In *Encyclopedia of Atmospheric Sciences*, 2nd ed.; Academic Press: Cambridge, MA, USA, 2015; Volume 2, pp. 196–200. [CrossRef]